

# Small Angle X-Ray Scattering Imaging of Soft Tissue by Using Laue Diffraction Optical System

Ge Jin<sup>1\*</sup>, Kenichi Okamura<sup>1</sup>, Yoshifumi Suzuki<sup>1</sup>, Yong Sun<sup>1</sup>, Yoshinori Chikaura<sup>1</sup>, Masami Ando<sup>2</sup>

<sup>1</sup>Department of Applied Science for Integrated System Engineering, Kyushu Institute of Technology, Kitakyushu, Japan

<sup>2</sup>Research Institute for Science and Technology, Tokyo University of Science, Noda, Japan

Email: \*jinge3139581@gmail.com

**How to cite this paper:** Jin, G., Okamura, K., Suzuki, Y., Sun, Y., Chikaura, Y. and Ando, M. (2018) Small Angle X-Ray Scattering Imaging of Soft Tissue by Using Laue Diffraction Optical System. *Open Journal of Medical Imaging*, 8, 54-63. <https://doi.org/10.4236/ojmi.2018.83007>

**Received:** February 26, 2018

**Accepted:** September 3, 2018

**Published:** September 6, 2018

Copyright © 2018 by authors and Scientific Research Publishing Inc. This work is licensed under the Creative Commons Attribution International License (CC BY 4.0).

<http://creativecommons.org/licenses/by/4.0/>



Open Access

## Abstract

We performed a feasibility study of Small angle X-ray scattering imaging under the condition of X-ray bright field imaging by Laue crystal diffraction optics of X-ray dark-field imaging that works as an angular analysis. Collagen in chicken tibia containing abundant soft fibrous tissue was chosen as a specimen. In traditional Small angle X-ray scattering optical system, we can derive the structure information of sample by calculating  $q$  value which is available from a scattering pattern. Thus it is usually necessary to conduct a 2D scan in order to obtain scattering image. In this paper it is described by a method by which not only small angle X-ray scattering imaging is available directly but also bright-field imaging and dark-field imaging can be obtained at the same time. As the first step, the feasibility of the imaging method should be confirmed by taking pictures of the samples with known periodic length. The preliminary test showed that the collagen's lattice spacing  $d$  is 65.1 nm that was also taken photos by scanning electron microscopy. By rotating Laue angular analyzer by 112 arcseconds small angle X-ray scattering image appeared in bright-field.

## Keywords

XDFI, SAXS, Synchrotron Radiation, Soft Tissue

## 1. Introduction

When the X-rays pass through the object, three kinds of interactions mainly occur such as absorption, refraction, scattering (small angle scattering and Compton scattering). Since the discovery of X-ray by Roentgen, absorption contrast imaging [1] [2] based on absorption principle has playing an important role in so many fields in the past hundred years. In recent years a lot of attention from

medical imaging and material characterization has been paid to refraction phase-contrast imaging [3].

Refraction phase contrast imaging has two advantages over absorption contrast: it can provide high contrast in soft tissue including articular cartilage and it can relatively suppress radiation dose. This X-ray imaging technology is applicable to medical diagnosis, performance evaluation of biomaterials and so on. Articular cartilage, ligament, cancer tissue and atherosclerotic plaque in blood cell that has very low X-ray absorption contrast so that one can not easily see these. There is drawback of X-ray absorption contrast in muscle and cancer tissue imaging so that these provide a very weak contrast. In order to solve this problem usually X-ray energy has been reduced substantially that might induce higher radiation dose. On the other hand articular cartilage whose main component is Ca is relatively low Ca concentration but this tissue is surrounded by high Ca concentration trabeculars so that there is no clear technique to visualize this under X-ray absorption contrast.

We are developing X-ray optical system called X-ray dark-field imaging (XDFI) [4]. This comprises two optical components: monochromator-collimator (MC) that provides with highly collimated X-ray beam with divergence of  $2.5 \times 10^{-7}$  rad and Laue angular analyzer (LAA) that has angular acceptance of  $3.85 \times 10^{-6}$  rad. This system that is a function of over all the radiation source, the degree of parallelity of the beam incident that can be made by adoption of MC onto specimen, thickness of LAA and the pixel size of CCD camera has reached till now the spatial resolution of approximately 10  $\mu\text{m}$ . The divergence of outgoing beam is at order of  $10^{-7}$  rad. So far XDFI has got success of viewing a variety of internal organs such as breast cancer, articular cartilages of finger, knee and shoulder, eye ball and blood cells such as iliac artery and coronary artery without staining with contrast agent in pathological way [5] [6].

This has brought us an image of scattering quite different from absorption based images. On the other hand, biological object usually contains long-period nanometer-scale structures. Due to the low crystallinity of this long period structure and a low X-ray absorptivity leading a low intensity, it becomes difficult to obtain a scattered image. In traditional small angle X-ray scattering (SAXS) optical system, e.g. Bonse-Hart system [7] and Kratky system [8], we can derive the structure information of sample by calculating  $q$  value which is available from a scattering pattern. Thus it is usually necessary to conduct a 2D scan in order to obtain scattering image. A small angle X-ray scattering topography [9] [10] that was proposed by Yoneda and Chikaura first in 1981 was used for visualizing internal periodic structure distribution of some biomaterials by mapping differences of small angle scattering.

In the paper, we study a new method to take a photo of small angle scattering imaging by rotating the Laue angular analyzer to exact scattering part by XDFI optical system. Not only SAXS imaging could be obtained directly, but also absorption contrast imaging, BFI imaging and DFI imaging the four kinds of im-

aging can be obtained and compared with each other. In the application aspect, at the first the feasibility of the imaging method should be confirmed by taking pictures of the periodic length known samples. It is expected that revealing the genesis of soft tissue lesions by visualization of subtle structures and becoming a useful tool for medical imaging in future.

## 2. Experiment and Principle

### 2.1. Preliminary Experiment

Preliminary test was performed at BL14B at Photon Factory before SAXS experiment at BL14C using XDFI optics. This was done in order to measure d-value spacing of fibers of collagen specimen and to estimate exposure time of the collagen specimen by the SAXS intensity. The angular position of the X-ray image of collagen with spacing of 65 nm should meet the angular information of SAXS. This system uses synchrotron X-ray produced at a 5 T vertical wiggler installed in the 2.5 GeV storage ring at Photon Factory, KEK in Tsukuba, Japan.

SAXS image corresponds to that taken at angular position calculated by the spacing 65 nm. Precision measurement of the spacing is very crucial; unless otherwise we cannot attain reasonable SAXS intensity. In order to obtain high incident intensity the asymmetric factor was reversely to condensate the beam intensity by making the beam size smaller so that the irradiated area has become 100  $\mu\text{m}$  instead of 5 mm as shown in **Figure 1**. Energy was adopted at 17.5 keV. Camera distance was set up to 850 mm. An Al needle of injector around 1mm diameter was used as beam stopper. Camera resolution was 7.4 pixel/ $\mu\text{m}$  with FOV 24 mm  $\times$  36 mm.

### 2.2. SAXS Imaging Experiment

The experiment was carried out at BL-14C station where optics is double-crystal

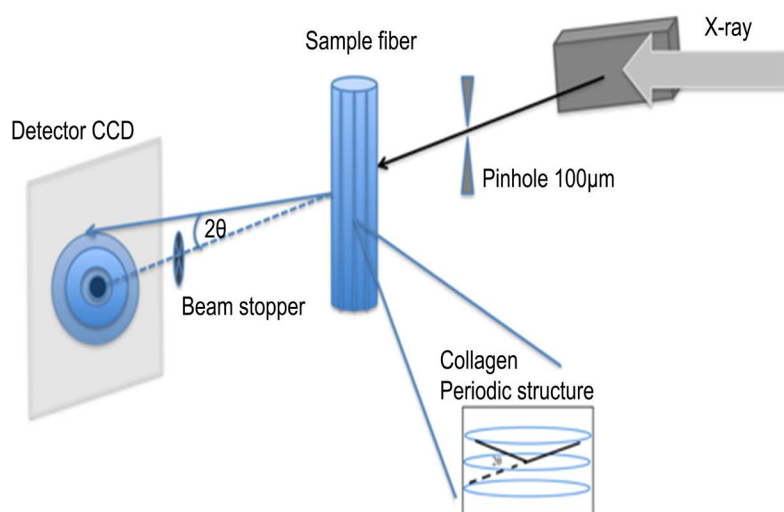


**Figure 1.** (Color online) Theoptical systemof auxiliary experiment for small angle scattering pattern of collagen.

monochromator 220 and mainly doing the bigger horizontal medical imaging station. Beam intensity of this station is approximately  $10^8$  photons/mm<sup>2</sup>/s at 33 keV. Vertically polarized white X-ray radiation at short wavelengths occurs from the super conducting wiggler that has a 5 T horizontal magnetic field. The size of the experimental hutch is 3.7 m (L) × 3.7 m (W) × 2.9 m (H), and height from the middle line of X-ray beams in the hutch is about 1360 mm. Beam size is V: 38 mm, H: 8 mm by design.

The X-ray optical system called X-ray dark-field is shown in **Figure 2**. There is an asymmetrically cut Bragg-case monochromator-collimator (MC), a sample rotational stage, LAA, and an X-ray CCD camera. As X-ray beam that has already been monochromated by a double-crystal monochromator up stream, called pre-monochromator, in the optical hutch is incident on MC with the incident grazing angle of  $\theta_B - \alpha$  where  $\theta_B$  is the Bragg angle and  $\alpha$  is the angle between the crystal surface and the diffracting planes. Due to this process, the MC expands the size of incident X-ray beam by a factor of  $1/b = \sin(\theta_B + \alpha) / \sin(\theta_B - \alpha)$ . Also the divergence of the outgoing beam becomes smaller compared to the intrinsic one by a factor  $\sqrt{b}$ .

X-ray is irradiating a sample, the phase shift happens at internal boundary of tissue so that the traveling direction changes. Utilizing this principle, the X-ray phase contrast occurs. It becomes possible to visualize the structure even regard to X-rays for the low absorption part such as living tissues. The X-ray phase contrast imaging is a method that detects the X-ray refraction of substance by utilizing the diffraction of the LAA which is installed after the sample. The diffraction occurs when the incident angle is at  $\theta_B$  formed between the background beam and the crystal lattice plane. After beam pass through LAA it will split into two waves such as forward diffraction wave and diffraction wave and dark field imaging and bright field imaging are obtained when put a sample into optic as shown in **Figure 2**.

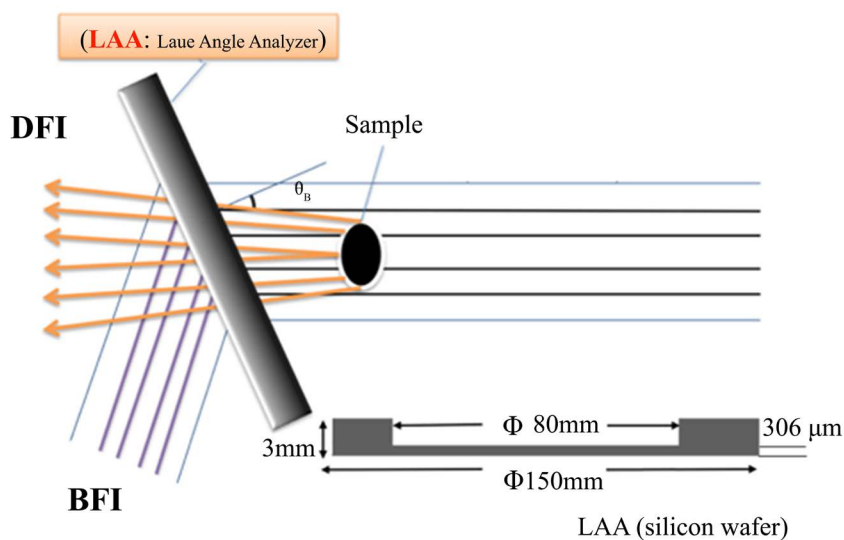


**Figure 2.** (Color online) Laue diffraction of X-ray dark field.

We used a chicken's leg (collagen  $d \approx 65$  nm) available from market to make into a specimen by size  $1 \text{ mm} \times 7 \text{ mm}$  after drying. Collagen and silver docosanoate with a chemical form of  $\text{C}_{22}\text{H}_{43}\text{AgO}_2$  ( $d \approx 5.8$  nm) usually were used as a standard sample with calibrated  $q$  value  $\left(q = \frac{2\pi}{d} = \frac{4\sin\theta}{\lambda}\right)$  in small-angle scattering experiment. Camera distance  $L = 750$  mm and the X-ray energy  $E = 17.5$  keV were adopted. Under this condition, it was calculated that collagen corresponding to the Bragg angle is  $112^\circ$  by the Bragg's law. Adjusting the optical system at  $w = 2\Lambda \sin_b(\theta - \theta_B - \Delta\theta_0)/\lambda = 0$ , where  $\Lambda = \lambda\chi \cos\theta_B/|P||\chi_\Gamma|$  is the Pendellosung fringe distance,  $P$  the polarization factor,  $\lambda$  the X-ray wavelength,  $\chi_\Gamma = -r_e\lambda^2 F_G / \pi V_C$  the polarizability, where  $r_e$  is the classical radius of electron,  $F_G$  the crystal structure form factor,  $V_C$  the volume of unit cell,  $\theta$  the angle that deviated from the Bragg angle  $\theta_B$  and  $\Delta\theta_0$ ,  $\theta = \theta_B - \Delta\theta_0$ , correction of the Bragg angle due to refraction expressed as  $\Delta\theta_0 = 2(1-n)/\sin 2\theta_B$  shown in **Figure 3**. Signal to noise ratio at DFI,  $S/N + \sqrt{N}|DFI$  is much smaller than that at BFI,  $S/N + \sqrt{N}|BFI$  so that one cannot expect a high quality of image using DFI. In order to have higher S/N image a BFI image without specimen at the angular position where small-angle scattering image was taken was subtracted from the sample image. Then we only attempted in BFI at position of  $b$  (outside of figure) where in the case of collagen 11,200 pulses.

The horizontal axis unit is arcsecond, and 100 pulse equals 1 arcsecond. When the X-rays pass through the object, three kinds of interactions mainly occur such as absorption, refraction, scattering (small angle scattering and Compton scattering). According to the above three physical phenomena, the beams which belong to different angle's order can be distinguished by rotating LAA. In the

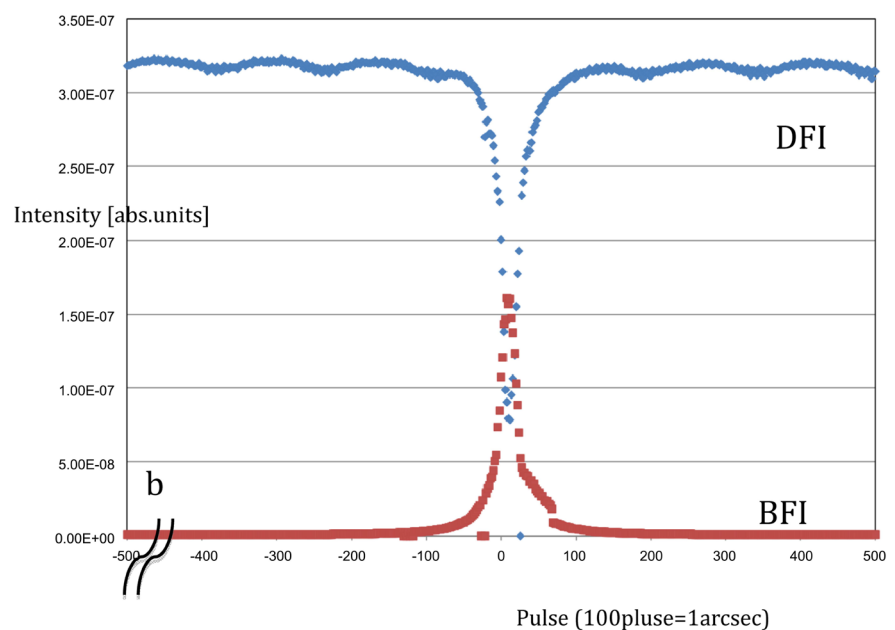


**Figure 3.** (Color online) Rocking curves of  $170 \mu\text{m}$  thickness of LAA.

case of X-ray, the refraction index is defined by  $n = 1 - i\beta - \delta$ . The real part  $\delta$  relate to refraction angle is  $10^{-5}$  radian which almost belongs 0.01% degree range. The small angle scattered beam belongs 1% degree to several degrees in the order of the angle range. Refraction beam with a relatively small angle can be analyzed and visualized by LAA, then the range of small angle scattering that is hundred times larger than it should be able to be analyzed. Many living organisms comprise collagen, and collagen has very low sensitivity in the absorption contrast image. And collagen is usually composed of a large number of light elements and periodic structure, therefore it is considered to be suitable for photographing both refraction phase contrast imaging and small-angle scattering imaging as a sample. To establish the imaging technique of small-angle scattering image, at the first stage, we did an experiment by using XDFI optics with spatial resolution of 8  $\mu\text{m}$ . Exposure time for refraction beam was around 50 seconds while that for scattering beam was 60 min.

### 3. Result

The result of the preliminary test in **Figure 4** showed that A position is direct beam, B is the first order diffraction and C is the second order diffraction. From A to B there are almost 125 pixels. The lattice spacing  $d$  is 65.1 nm. This means by rotating LAA by 112 arcseconds SAXS image should appear. The SAXS intensity is expected to be approximately 1/120,000 of the incident X-ray intensity. This has made us possible to estimate the exposure time of SAXS image so that it is about 10 min. As shown in **Figure 5** dark-field imaging, bright-field imaging, SAXS imaging 112 arcseconds apart from the just Bragg angle were confirmed.

X-ray contrast image of collagen at chicken tibia appeared when the periodicity matched the X-ray Bragg condition.

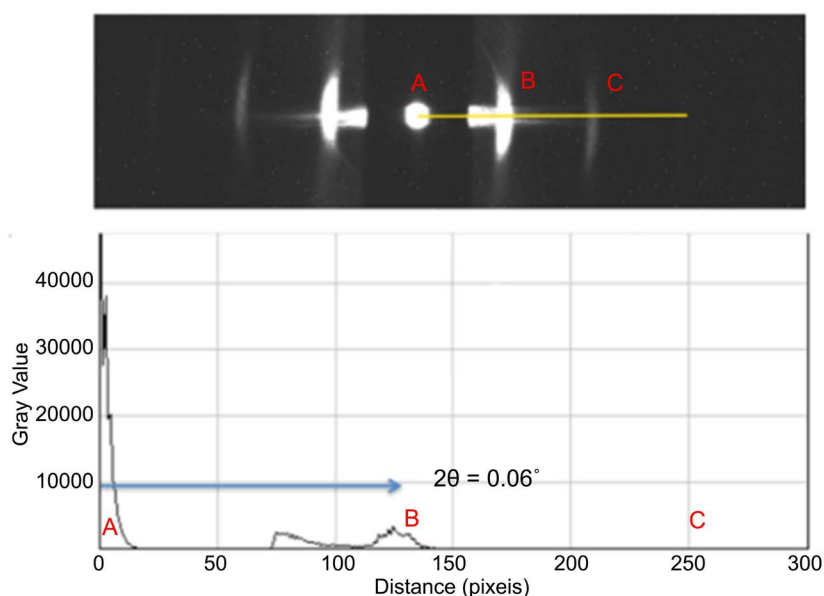


**Figure 4.** (Color online) Small angle scattering pattern of collagen.

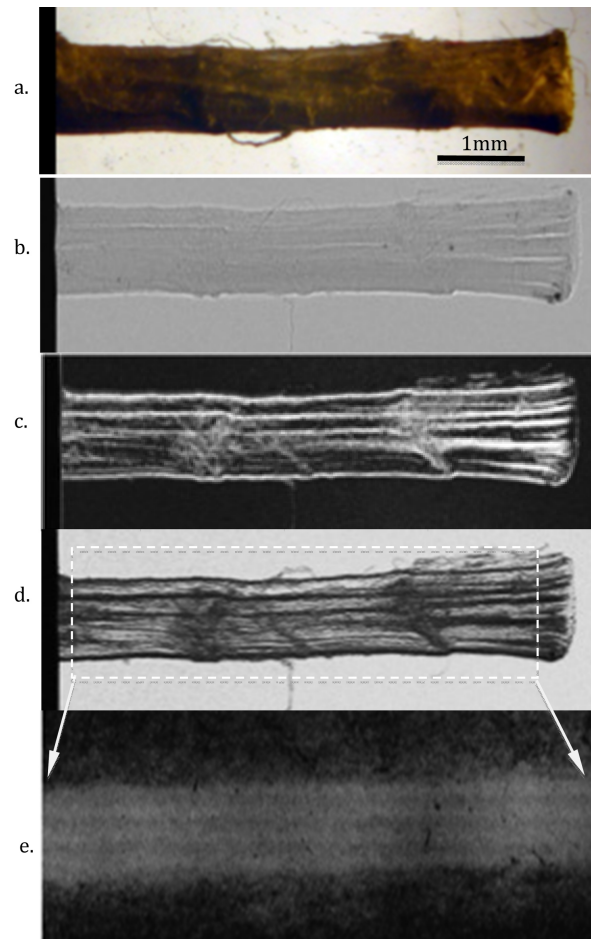


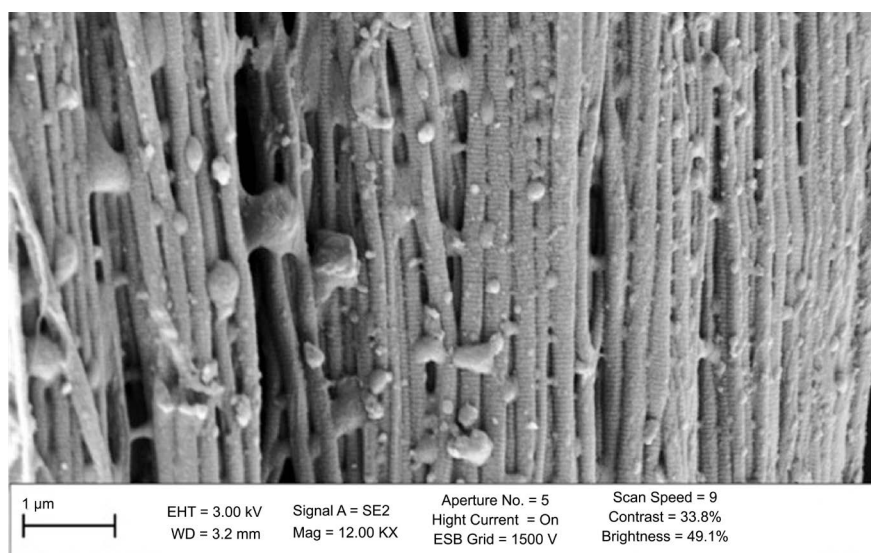
**Figure 5.** (Color online) The result of various kinds of imaging. (a) Optical microscope; (b) Absorption imaging; (c) DFI imaging; (d) BFI imaging; (e) SAXS imaging.

#### 4. Discussion

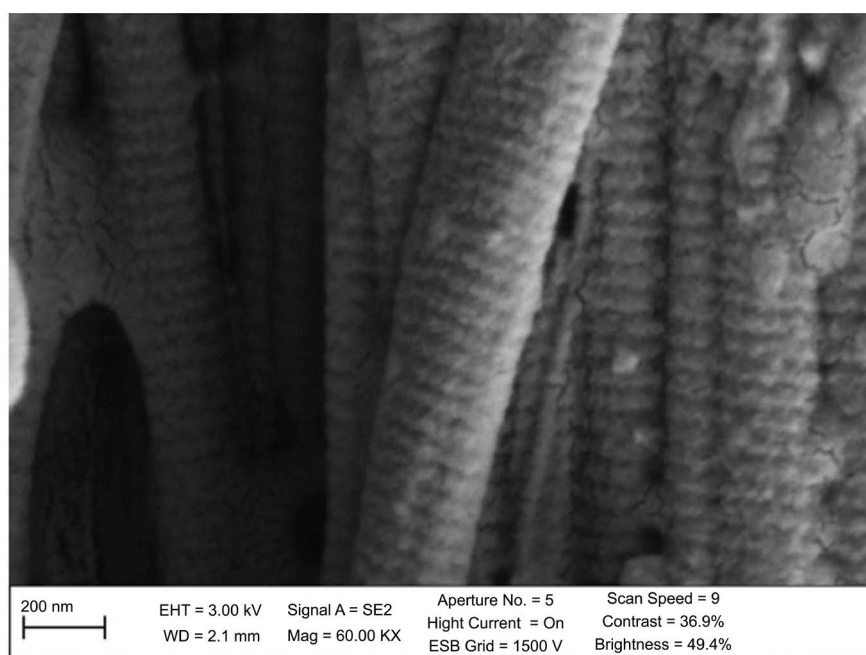
It has become clear that SAXS image can be taken under the XDFI optical system. In order to increase the X-ray intensity delivered to specimen that is relating to shortening of exposure time one could introduce a bent crystal or asymmetric crystal with  $b \ll 1$ . Under this condition due to angular distribution of crystallite of the specimen and its physical size the above consideration can work.

In order to obtain internal structure of collagen to confirm the results of small-angle scattering image, we took electron microscopic images of scanning electron microscopy (SEM). And the result of 65 nm periodic length shown in SEM image is corresponding to the diffraction pattern in preliminary test and SAXS imaging in **Figure 5(e)**.

As shown in **Figure 6(a)** it is clear that collagen is formed by a lot of fine fibres, while the transversal structure has more random fiber arrangement. We can easily understand that this periodicity in **Figure 6(b)** gives rise to diffraction when this structure satisfies the Bragg condition for the X-rays with certain wavelength.



(a)



(b)

**Figure 6.** SEM images of chicken collagen's structure by different magnification.

CCD camera that has pixel size of 7.4 μm cannot observe the nanometer order of collagen structure itself. This means that the contrast observed in X-ray imaging in **Figure 5(e)** provides us information of local distribution of periodicity of collagen around 65 nm.

X-ray absorption contrast shows difference of absorption at local point of material, while that of refraction contrast is dependent on local electron density distribution.

There should be a rocking curve corresponding to collagen 65 nm at the position of the LAA rotated to 112 arcseconds. Although **Figure 5(e)** may be not



taken just at the peak position of the RC, the intensity is already strong enough to show the periodic structure. On the other hand, even if the images were taken along RC with different periods position, due to the resolution, an obvious change of image in brightness reflecting the distribution of different periodic positions at different part of the sample cannot be expected under current conditions. A precision sample turntable for scanning the peak of the small angle scattering and a CCD camera of which the field of view does not have to be large but higher resolution is needed in the future experiment.

## 5. Conclusions

We have successfully achieved a novel technique of viewing inside collagen of chicken tibia by use of SAXS. The achievement tells us that BFI of XDFI can provide us with SAXS image. In view of exposure time and angular resolution in SAXS image we could have advanced this technique based on the system developed by Yoneda and Chikaura.

With approach by taking three images such as phase-contrast one, absorption one and SAXS this system proposed here can be a powerful tool to analyze structure of a specimen. Nevertheless there is still a space to improve the quality of X-ray images. For instance one can introduce vacuum tube for X-ray path to reduce scattering source and reduce beam quality towards the spherical beam rather than a parallel beam.

In the next step we could proceed onto a more complicated unknown structure of biomaterial. Thus we can expect that each X-ray image can tell different components of material.

As a conclusion we could foresee application of SAXS image to pathological diagnosis to see 3-dimensional distribution of soft tissue of biomaterial and nanomaterial.

## Conflicts of Interest

The authors declare no conflicts of interest regarding the publication of this paper.

## References

- [1] Momose, A. (2005) Recent Advances in X-Ray Phase Imaging. *Japanese Journal of Applied Physics*, **44**, 6355-6367. <https://doi.org/10.1143/JJAP.44.6355>
- [2] Takeda, T., Momose, A., Yu, Q., Wu, J., Hirano, K. and Itai, Y. (2000) Phase-Contrast X-Ray Imaging with a Large Monolithic X-Ray Interferometer. *Journal of Synchrotron Radiation*, **7**, 280-282. <https://doi.org/10.1107/S0909049500004295>
- [3] Chapman, D., Thomlinson, W., Johnston, R.E., Washburn, D., Pisano, E., Gmür, N. et al. (1997) Diffraction Enhanced X-Ray Imaging. *Physics in Medicine & Biology*, **42**, 2015-2025. <https://doi.org/10.1088/0031-9155/42/11/001>
- [4] Ando, M., Sugiyama, H., Maksimenko, A., Pattanasiriwisawa, W., Hyodo, K. and Zhang, X.W. (2001) A New Optics for Dark-Field Imaging in X-Ray Region "Owl". *Japanese Journal of Applied Physics*, **40**, L844. <https://doi.org/10.1143/JJAP.40.L844>

- 
- [5] Ando, M., Sunaguchi, N., Wu, Y., Do, S., Sung, Y., Louissaint, A., Yuasa, T., Ichihara, S. and Gupta, R. (2013) X-Ray Phase Contrast Imaging in the Dark Field: Implementation and Evaluation Using Excised Tissue Specimens. *European Radiology*, **23**, 3021-3029.
- [6] Ando, M., Maksimenko, A., Yuasa, T., Hashimoto, E., Yamasaki, K., Ohbayashi, C., Sugiyama, H., Hyodo, K., Kimura, T., Esumi, H., Akatsuka, T., Li, G., Xian, D., Ueno, E., Bando, H., Ichihara, S., Endo, T., Moriyama, N. and Nishino, H. (2006) 2D and 3D Visualization of Ductal Carcinoma *in Situ* (DCIS) Due to X-Ray Refraction Contrast. *Bioimages*, **14**, 1-8.
- [7] Bonse, U. and Hart, M. (1966) Small-Angle X-Ray Scattering. In: Brumberger, H., Ed., Gordon and Breach, New York.
- [8] Glatter, G. and Kratky, O. (1982) Small Angle X-Ray Scattering. Academic Press, London.
- [9] Yoneda, Y. and Chikaura, Y. (1981) Polycrystal Scattering Topography, Scattering Tomography and Their Perspective Fields of Application. *Japanese Journal of Applied Physics*, **37**, 412-418.
- [10] Yoneda, Y. and Chikaura, Y. (1982) Scattering Tomography. *Japanese Journal of Applied Physics*, **21**, L31-L33. <https://doi.org/10.1143/JJAP.21.L31>